Amphiphilic Templating of Mesostructured Zirconium Oxide

Michael S. Wong and Jackie Y. Ying*

Department of Chemical Engineering, Massachusetts Institute of Technology, Cambridge, Massachusetts 02139

Received July 23, 1997. Revised Manuscript Received June 15, 1998

The synthesis of zirconium oxide with a mesostructured framework (Zr-TMS) has been achieved through the use of amphiphilic compounds with a variety of headgroups (anionic and nonionic) and tail group chain lengths (1−18 carbons). Anionic surfactants with phosphate, carboxylate, sulfate, and sulfonate headgroups led to disordered hexagonal and/or layered phases. Mesoporous zirconia with high surface areas could be obtained through calcination of materials templated with phosphate amphiphiles; the phosphate headgroups remained on the pore walls and appeared necessary for thermal stability. Nonionic amine amphiphiles have been found to lead to less ordered zirconia mesostructures, due to the weak interaction with the zirconium *n*-propoxide precursor. The chain-length-independent templating ability of the amphiphiles and ex situ ^{31}P MAS NMR of dodecyl phosphate (before and after incorporation into Zr-TMS) supported a method of formation involving covalent-bond interactions between the headgroup and the inorganic precursor.

Introduction

The discovery of the M41S family of silicate mesoporous molecular sieves has fueled great interest in this new class of materials, particularly in MCM-41.[1,2] MCM-41 has hexagonally packed cylindrical pore channels with surface areas greater than 1200 m^2/g and uniform pore sizes that can be tailored from 20 to 100 Å in diameter, making for attractive heterogeneous catalysts, catalyst supports, and nanocomposite host materials for a wide range of applications.[3−5] The ability to synthesize these materials and to control the structural characteristics on a mesoscopic scale stems from the unique synthesis route of the so-called "liquid-crystal templating" (LCT) method, in which a surfactant solution is contacted with a silicate salt solution. The LCT method relies on (i) the electrostatic interaction between the positively charged ammonium headgroup of the surfactant and the negatively charged silicate species and (ii) the assembly of the surfactant molecules into micellar rods, around which the silicates form a continuous, solid, mesostructured material. The surfactants can be removed through calcination, leaving behind the hexagonally packed mesoporous silicate framework of MCM-41.

MCM-41-type materials composed of transition metal oxides have been sought recently.[6−12,14−26] Transition metal oxides play an important role as industrial catalysts and catalyst supports, but they are typically available with relatively low surface areas and poorly defined pore structures. A number of non-silicate MCM-

* To whom correspondence should be addressed.

(1) Kresge, C. T.; Leonowicz, M. E.; Roth, W. J.; Vartuli, J. C.; Beck, J. S. *Nature* **1992**, *359*, 710.
(2) Beck, J. S.; Vartuli, J. C.; Roth, W. J.; Leonowicz, M. E.; Kresge, C. T.; Schmitt, K. D.; Chu, C. T.-W.; Olsen, D. H.; Sheppard, E. W.; McCullen, S. B.; Higgins, J. B.; Schlenker, J. L. *J. Am. Chem. Soc.* **1992**, *114*, 10834.
(3) Wu, C.-G.; Bein, T. *Chem. Mater.* **1994**, *6*, 1109.
(4) Bowes, C. L.; Malek, A.; Ozin, G. A. *Chem. Vap. Deposition* **1996**, *2*, 97.
(5) Sayari, A. *Chem. Mater.* **1996**, *8*, 1840.
(6) Huo, Q.; Margolese, D. I.; Ciesla, U.; Demuth, D. G.; Feng, P.; Gier, T. E.; Sieger, P.; Firouzi, A.; Chmelka, B. F.; Schüth, F.; Stucky, G. D. *Chem. Mater.* **1994**, *6*, 1176.
(7) Huo, Q.; Margolese, D. I.; Ciesla, U.; Feng, P.; Gier, T. E.; Sieger, P.; Leon, R.; Petroff, P. M.; Schüth, F.; Stucky, G. D. *Nature* **1994**, *368*, 317.
(8) Ciesla, U.; Demuth, D.; Leon, R.; Petroff, P.; Stucky, G.; Unger, K.; Schüth, F. *J. Chem. Soc., Chem. Commun.* **1994**, 1387.
(9) Abe, T.; Taguchi, A.; Iwamoto, M. *Chem. Mater.* **1995**, *7*, 1429.
(10) Stein, A.; Fendorf, M.; Jarvie, T. P.; Mueller, K. T.; Benesi, A. J.; Mallouk, T. E. *Chem. Mater.* **1995**, *7*, 304.
(11) Janauer, G. G.; Dobley, A.; Guo, J.; Zavalij, P.; Whittingham, M. S. *Chem. Mater.* **1996**, *8*, 2096.
(12) Ulagappan, N.; Rao, C. N. R. *Chem. Commun.* **1996**, 1685.
(13) Although the term "mesostructured" formally refers to both surfactant-containing and surfactant-free materials, in this paper it will solely refer to the former.
(14) Antonelli, D. M.; Ying, J. Y. *Angew. Chem., Int. Ed. Engl.* **1995**, *34*, 2014.
(15) (a) Antonelli, D. M.; Ying, J. Y. *Angew. Chem., Int. Ed. Engl.* **1996**, *35*, 426. (b) Antonelli, D. M.; Nakahira, A.; Ying, J. Y. *Inorg. Chem.* **1996**, *35*, 3126.
(16) Antonelli, D. M.; Ying, J. Y. *Curr. Opin. Colloid Interface Sci.* **1996**, *1*, 523.
(17) Antonelli, D. M.; Ying, J. Y. *Chem. Mater.* **1996**, *8*, 874.
(18) Bagshaw, S. A.; Pinnavaia, T. J. *Angew. Chem., Int. Ed. Engl.* **1996**, *35*, 1102.
(19) Vaudry, F.; Khodabandeh, S.; Davis, M. E. *Chem. Mater.* **1996**, *8*, 1451.
(20) Tian, Z.-R.; Tong, W.; Wang, J.-Y.; Duan, N.-G.; Krishnan, V. V.; Suib, S. L. *Science* **1997**, *276*, 926.
(21) Terribile, D.; Trovarelli, A.; de Leitenburg, C.; Dolcetti, G.; Llorca, J. *Chem. Mater.* **1997**, *9*, 2676.
(22) Liu, P.; Liu, J.; Sayari, A. *Chem. Commun.* **1997**, 577.
(23) Ciesla, U.; Schacht, S.; Stucky, G. D.; Unger, K. K.; Schüth, F. *Angew. Chem., Int. Ed. Engl.* **1996**, *35*, 541.
(24) Liu, P.; Reddy, J. S.; Adnot, A.; Sayari, A. *Mater. Res. Soc. Symp. Proc.* **1996**, *431*, 101.
(25) Wong, M. S.; Antonelli, D. M.; Ying, J. Y. *Nanostr. Mater.* **1997**, *9*, 165.
(26) For example: (a) Hudson, M. J.; Knowles, J. A. *J. Mater. Chem.* **1996**, *6*, 89. (b) Pacheco, G.; Zhao, E.; Garcia, A.; Sklyarov, A.; Fripiat, J. J. *Chem. Commun.* **1997**, 491.

S0897-4756(97)00525-5 CCC: $15.00
Published on Web 07/22/1998

41-type *mesostructured*[13] materials, e.g., oxides of antimony, iron, molybdenum, tin, vanadium, and chromium,[6−12] were prepared through a generalized electrostatic approach. These materials, however, only maintain the mesostructure in the presence of the templating surfactant molecules, the removal of which will collapse the mesostructure so that well-defined porous structures of these metal oxides are not attained via such preparation. Through a number of alternative surfactant-assisted synthesis approaches, *mesoporous* non-silicate materials have been achieved, e.g., titania,[14] niobia,[15,16] tantala,[17] alumina,[18,19] manganese oxide,[20] ceria,[21] hafnia,[22] and zirconia.[23−26]

Of the transition metal oxides, zirconium oxide is of particular interest for acid catalysis.[27] Zirconium oxide contains both weakly acidic and basic surface sites, providing for high activity in reactions requiring acid−base bifunctional catalysts.[28,29] Porous zirconia with high BET (Brunauer−Emmett−Teller) surface areas (100−200 m^2/g) can be made by chemical precipitation and supercritical drying of zirconia gels.[30] An inherent drawback of these materials, however, is the facile sinterability and concomitant loss of surface area at elevated temperatures (>400 °C). The major thermodynamic driving force is the crystalline transformation of these zirconia materials to dense, low-surface-area monoclinic and metastable tetragonal phases.[31] By introducing dopants, such as phosphates[32] and sulfates,[33] the relatively low thermal stability of pure zirconia can be improved. Also, modified zirconia exhibits higher acid strength and activity for acid-catalyzed reactions; for example, phosphated zirconia is mildly acidic and sulfated zirconia is strongly acidic or even "superacidic".[32,33]

There has been great interest, therefore, in preparing mesoporous zirconium oxide with high surface area via the surfactant templating route. Some synthetic approaches have been based upon the concepts of electrostatic,[6,7] hydrogen-bonding,[34] and covalent-bond interactions,[15,17] but more often than not, they have resulted in a lamellar phase.[35] Removal of the surfactant without collapse of the zirconium oxide framework is not possible in most cases; the few exceptions are microporous "zirconium oxophosphate"[23,24] and zirconium oxide,[23] and mesoporous phosphated zirconia.[25] Other methods that lead to porous zirconia-based materials have engaged surfactants in a nontemplating role, whereby the surfactants do not self-assemble to result in well-defined mesostructures.[26]

Our previous investigation on the preparation of mesoporous phosphated zirconia[25] has suggested the flexibility of extending the covalent-bond approach to other templating agents. In this paper, we examined the synthesis of mesostructured zirconium oxide via the covalent-bond approach with a variety of surfactants. We found that mesostructured zirconium oxide could be prepared with anionic and nonionic surfactants, but the attainment of stable, well-defined mesoporous structures was highly dependent on the nature of the headgroup. Mesostructured zirconium oxide could also be prepared with short-chained templating molecules too small to be regarded as true surfactants.

Experimental Section

Chemicals. Anionic and nonionic amphiphilic compounds were used in the synthesis of mesostructured zirconium oxide. Here, the term "amphiphile" refers to surface-active compounds containing, within the same molecule, a hydrophilic headgroup and a hydrophobic hydrocarbon tail group of any carbon chain length; amphiphiles are generally considered surfactants when the tail group contains eight carbons or more.[36] Carboxylate amphiphiles ($C_nH_{2n+1}COO^-$, $n/2 = 0.5$, 1−9) were obtained from Aldrich Chemical (Milwaukee, WI) and were used without further purification. Dodecyl sulfate surfactant ($C_nH_{2n+1}SO_4^-$, $n = 12$) and alkylsulfonate surfactants ($C_nH_{2n+1}SO_3^-$, $n = 6$, 16) were obtained in sodium salt form from Aldrich.[37] Primary amine amphiphiles ($C_nH_{2n+1}NH_2$, $n = 4$, 6, 12) were purchased from Aldrich. Phosphate compounds ($C_nH_{2n+1}PO_4^{2-}$, $n = 4$, 8, 12, 16) were either synthesized[38] or obtained from Lancaster Synthesis (Windham, NH) and Johnson Matthey Alfa Aesar (Ward Hill, MA). Swelling agents (cyclohexane and toluene) and chelating agents (acetylacetone) were purchased from Aldrich. The *n*-propoxide form of zirconium alkoxide was used in this study, and it was introduced in a *n*-propanol solution [74 wt % zirconium tetrakis(*n*-propoxide)]. Zirconium ethoxide (99+%) and isopropoxide (99+%) were also used in some experiments. The alkoxides were commercially available from Aldrich and Strem Chemicals (Newburyport, MA) and were used without further purification.

Synthesis. In the covalent-bond approach, the synthesis of mesostructured zirconium oxide began with the addition of a molar equivalent (unless otherwise stated) of amphiphilic compound to the zirconium *n*-propoxide solution. Zirconium *n*-propoxide is hygroscopic and can precipitate out of solution prematurely if care is not taken to minimize exposure to air. The mixture was quickly stirred at room temperature until the amphiphile dissolved completely. It could be heated briefly to help solubilize undissolved surfactants. Swelling agents, if any, were added at this point. Precipitation began almost immediately after deionized water was added to the solution, and the resulting mixture was stirred for 1 h under ambient conditions. The mixture was then left to stand overnight, before aging at 80 °C for 4 days. After the aging step, the precipitate was filtered and washed with deionized water three times. The white to yellowish-white powder was finally air-dried overnight under a hood.

When alkyl phosphate amphiphiles were used, precipitation occurred without the water addition step due to the loss of solubility of oligomerized zirconium precursor. The resulting mixture was vigorously stirred until a moist, cream-colored intermediate was obtained. Water was then added, and the mixture was stirred for 0.5 h and left under static conditions overnight before aging at elevated temperatures.

(27) Yamaguchi, T. *Catal. Today* **1994**, *20*, 199.
(28) Nakano, Y.; Iizuka, T.; Hattori, H.; Tanabe, K. *J. Catal.* **1979**, *57*, 1.
(29) Tanabe, K.; Yamaguchi, T. *Catal. Today* **1994**, *20*, 185.
(30) Ward, D. A.; Ko, E. I. *Chem. Mater.* **1993**, *5*, 956.
(31) Subbarao, E. C. In *Science and Technology of Zirconia*; American Ceramic Society: Columbus, OH, 1981; p 1.
(32) Boyse, R. A.; Ko, E. I. *Catal. Lett.* **1996**, *38*, 225.
(33) (a) Jin, T.; Yamaguchi, T.; Tanabe, K. *J. Phys. Chem.* **1986**, *90*, 4794. (b) Davis, B. H.; Keogh, R. A.; Srinivasan, R. *Catal. Today* **1994**, *20*, 219. (c) Song, X.; Sayari, A. *Catal. Rev.-Sci. Eng.* **1996**, *38*, 329.
(34) (a) Tanev, P. T.; Pinnavaia, T. J. *Science* **1995**, *267*, 865. (b) Bagshaw, S. A.; Prouzet, E.; Pinnavaia, T. J. *Science* **1995**, *269*, 1242. (c) Tanev, P. T.; Pinnavaia, T. J. *Chem. Mater.* **1996**, *8*, 2068.
(35) For example: (a) Weidenhof, V.; Gropper, F.; Müller, U.; Marosi, L.; Cox, G.; Houbertz, R.; Hartmann, U. *J. Mater. Res.* **1997**, *12*, 1634. (b) Huang, Y.; Sachtler, W. M. H. *Chem. Commun.* **1997**, 1181. (c) Kim, A.; Bruinsma, P.; Chen, Y.; Wang, L.-Q.; Liu, J. *Chem. Commun.* **1997**, 161.
(36) Moroi, Y. *Micelles: Theoretical and Applied Aspects*; Plenum Press: New York, 1992.
(37) All but the sulfur-containing anionic amphiphiles are protonated.
(38) Nelson, A. K.; Toy, A. D. F. *Inorg. Chem.* **1963**, *21*, 775.

To reduce the reactivity of the zirconium precursor in certain experiments, 1 molar equiv of acetylacetone was added slowly to zirconium *n*-propoxide, producing zirconium acetylacetonate tris(*n*-propoxide).[39] Heat was generated by the reaction and the resulting solution was orange-colored. Amphiphilic compounds were then added to this zirconium chelate as 5 wt % aqueous solutions. These steps comprise the modified sol−gel method, as reported in the synthesis of Ti-TMS1.[14]

Surfactant Template Removal. Unless otherwise noted, the as-synthesized material was calcined at 400 °C under flowing nitrogen for 3 h and then under air for another 3 h, after a ramp rate of 2 °C/min. From differential thermal analysis (DTA) experiments, calcination under air is exothermic due to the combustion of organics; calcination under nitrogen is an endothermic process, as the organics undergo pyrolysis. Calcination was also carried out at higher temperatures. Depending on the amphiphiles used in the synthesis, alternative techniques in template removal included washing the powders with acidic and basic solutions (1.0−3.3 M solutions), and Soxhlet extraction in toluene.

Characterization. Powder X-ray diffraction (XRD) data were recorded on a Siemens D5000 diffractometer using nickel-filtered Cu Kα radiation with wavelength $\lambda = 1.5406$ Å. Diffraction patterns were collected under ambient conditions for $2\theta = 1.6-20.0°$ with a resolution of 0.04°.

Transmission electron micrographs (TEM) were taken on a JEOL 2000FX transmission electron microscope equipped with a lanthanum hexaboride (LaB_6) gun operating at an accelerating voltage of 200 kV and with an objective aperture of 50 μm. Samples for TEM studies were ground and supported on a carbon-coated copper grid.

Nitrogen adsorption−desorption isotherms were obtained at 77 K on a Micromeritics ASAP 2010 Gas Sorption and Porosimetry System. Samples were normally prepared for measurement by degassing at 150 °C under vacuum until a final pressure of 1×10^{-3} Torr was reached. BET surface areas were determined over a relative pressure range from 0.05 to 0.20.[40] Mesopore size distributions were calculated from the adsorption branch of the isotherms using the BJH (Barrett−Joyner−Halenda) method.[41]

Nonsimultaneous thermogravimetric analysis (TGA) and DTA were performed on a Perkin-Elmer Series 7 Thermal Analysis System. A ramp rate of 2 °C/min was used. Purified nitrogen, oxygen, and air were employed as the purge gases.

Fourier transform infrared (FTIR) spectroscopy was performed on a Bio-Rad FTS-60A/896 spectrometer. An MTEC Model 200 photoacoustic (PA) cell allowed nondestructive characterization of the powder samples. PA-FTIR spectra were collected at a scan speed of 5 kHz for wavenumbers of 400−4000 cm^{-1} with a resolution of 4 cm^{-1}. Samples were purged under a stream of helium (99.999+%).

Elemental analysis through inductively coupled plasma atomic emission spectroscopy (ICP-AES) was performed by Huffman Laboratories (Golden, CO). Solid-state ^{31}P magic angle spinning nuclear magnetic resonance (MAS NMR) spectra were collected at 109.55 MHz for ^{31}P resonance and at 270.62 MHz for proton decoupling by Spectral Data Services, Inc. (Champaign, IL). An 85% H_3PO_4 solution was used as the external reference.

Results and Discussion

The synthesis of mesostructured zirconium oxide was examined with anionic and nonionic amphiphilic compounds. Anionic amphiphiles contain multiple reactive oxygen atoms in the headgroup (e.g., phosphate, carboxylate, sulfate, and sulfonate), while the nucleophilic headgroups of the nonionic amphiphiles (e.g., amine) are capable of attacking the highly electrophilic zirconium atom in the alkoxide.[42] Figure 1 shows the typical XRD patterns for which surfactant-containing mesostructured zirconia materials termed Zr-TMS were found possible, as prepared through the covalent-bond route. Summarized in Table 1 are the *d* spacing values of zirconia mesostructures prepared with the various amphiphiles.

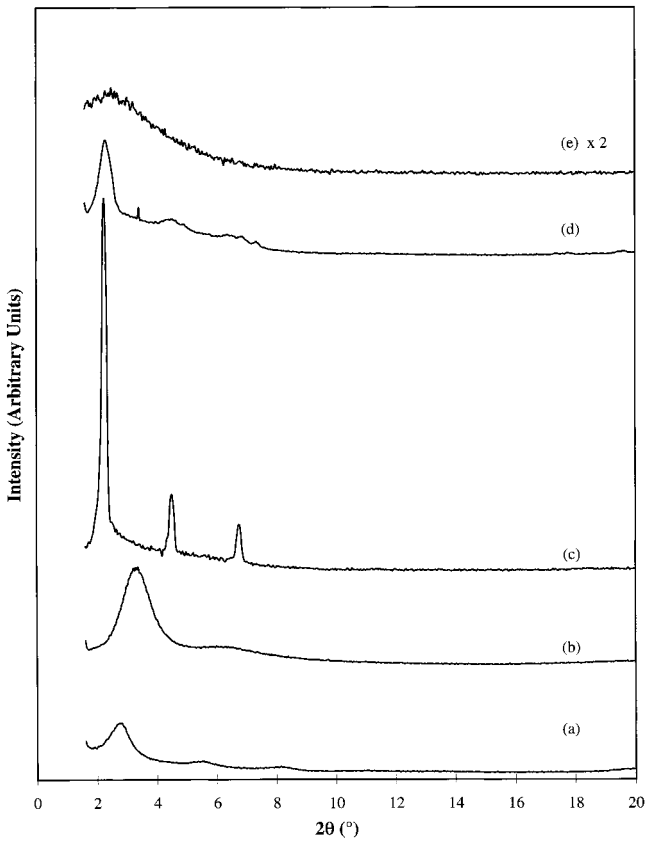

Figure 1. Typical XRD patterns of covalently bonded zirconia−surfactant Zr-TMS mesostructures prepared with (a) $C_{12}H_{25}PO_4^{2-}$, (b) $C_{12}H_{25}COO^-$, (c) $C_{12}H_{25}SO_4^-$, (d) $C_{16}H_{33}SO_3^-$, and (e) $C_{12}H_{25}NH_2$ amphiphiles as the templating agents.

Table 1. Measured d_{100} Spacings (Å) of Mesostructures Prepared with Amphiphiles of Various Headgroups and Chain Lengths

carbon number, *n*	headgroup				
	PO_4^{2-}	COO^-	SO_4^-	SO_3^-	NH_2
1		14.6			
2		15.4			
4	16.6	17.4			
6		20.4		17.0	
8	24.2	23.1			
10		26.2			
12	31.0	26.7	38.3		34.5
14		29.2			
16	38.4	31.3		35.0	
18		33.1			

Anionic Amphiphiles. *Phosphate Headgroup*. Alkyl phosphates are expected to be highly reactive with zirconium alkoxides. There are three nucleophilic oxygens in the headgroup capable of attacking multiple

(39) Debsikdar, J. C. *J. Non-Cryst. Solids* **1986**, *86*, 231.
(40) Gregg, S. K.; Sing, K. S. W. *Adsorption, Surface Area and Porosity*, 2nd ed.; Academic Press: London, 1982.
(41) Barrett, E. P.; Joyner, L. G.; Halenda, P. P. *J. Am. Chem. Soc.* **1951**, *73*, 373.
(42) Livage, J.; Henry, M.; Sanchez, C. *Prog. Solid St. Chem.* **1988**, *18*, 259.

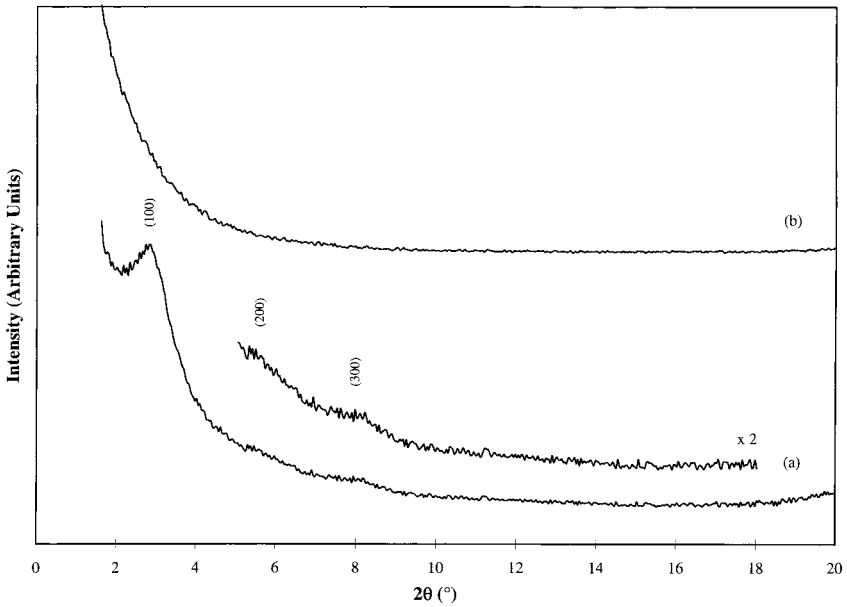

Figure 2. XRD patterns of Zr-TMS synthesized with $C_{12}H_{25}PO_4^{2-}$ via ligand-assisted templating route: (a) before and (b) after calcination.

zirconium alkoxide molecules. For example, phosphates (and phosphonates) are known to form layered crystalline materials with zirconium and other metal(IV) cations.[43] Dodecyl phosphate was combined with 1 molar equiv of zirconium *n*-propoxide, creating an intermediate prior to the addition of deionized water, giving a molar composition of 1.0:1.0:250.0 Zr:surfactant:H_2O. Deionized water was used instead of an acidic aqueous solution (pH = 1.2, HCl), as modified from our original procedure.[25] Aging at 80 °C for 96 h yielded a mesostructured material (Figure 2a), and the XRD pattern could be indexed to a lamellar phase (d_{100} = 31.0 Å), although the broadness of the peaks did not preclude the existence of a hexagonal phase. A lamellar-phase XRD pattern might also be exhibited by a material with tightly packed but randomly oriented pore channels.[44] Indeed, TEM studies have shown that as-synthesized Zr-TMS contained both lamellar (Figure 3a) and disordered hexagonal (Figure 3b) phases. Upon calcination, an X-ray amorphous material was obtained (Figure 2b), but the resulting mesoporous material was found to have a very high surface area (356 m^2/g) and a BJH pore size distribution between 20 and 40 Å, centered at ca. 25 Å (see Figure 6c for the nitrogen adsorption−desorption isotherm). The aging conditions were found to be optimal for producing high-surface-area, mesoporous materials. The modified sol−gel route led to zirconia mesostructures with lower surface areas and was not examined further.

The effect of the surfactant to zirconium *n*-propoxide molar ratio was studied. Vartuli et al.[45] reported that the following different phases of M41S materials could be obtained by varying the surfactant/silicon molar ratio: two-dimensional hexagonal *p*6*m* MCM-41 (<1:1), cubic *Ia*3*d* MCM-48 (1:1), and lamellar MCM-50 (1.2:1−1.8:1). At ratios approaching 2:1, a silicon-surfactant molecular compound was formed, instead of a condensed mesostructure. Antonelli et al.[15b] showed that different phases of Nb-TMS materials could also be obtained by adjusting the surfactant/niobium ratio: hexagonal *p*6*m* Nb-TMS1 (<0.75:1), three-dimensional hexagonal $P6_3/mmc$ Nb-TMS2 (1.25:1), and layered Nb-TMS4 (2:1). No distinct mesostructure phase dependence on surfactant-to-metal ratio was found in the zirconia system with dodecyl phosphate surfactants, however. Figure 4 shows the XRD patterns of materials prepared with increasing surfactant:zirconium molar ratios from 0.17:1 to 2:1. At ratios ≤ 0.5:1, the low-angle diffraction peaks were not found in the XRD patterns. The characteristic d_{100} peak appeared at a ratio of 0.75:1, and the higher order peaks became more noticeable at ratios ≥ 1:1. The d_{100} values were calculated to be ca. 31 Å and did not shift appreciably (±1 Å) with changing surfactant:metal ratios in the range of 0.75:1 to 2:1. Transitions between mesostructured phases, or "mesophases", might depend strongly on the framework's ability to restructure.[6] Recently, it was shown that MCM-48 can be prepared by aging freshly precipitated MCM-41 at 150 °C for several hours.[46] Ethanol evolved from the hydrolysis of the tetraethyl orthosilicate precursor was found to be necessary for the transformation of MCM-41 to MCM-48 to occur. In the case of Zr-TMS, *n*-propanol was present as the solvent for the zirconium *n*-propoxide and as the hydrolysis product of zirconium *n*-propoxide, but no similar phase transition was observed. This lack of mesophase transformation in Zr-TMS could be due to the existence of multiple bonds between the phosphate headgroup and the zirconium atom, locking in a preferred mesostructure.

Control of *d* spacings was achieved through the use of different alkyl phosphate chain lengths. The shifting of the main (100) peak toward lower 2θ angles with increasing tail group length could be observed in the

(43) Maya, L. *Inorg. Nucl. Chem. Lett.* **1979**, *15*, 207. (b) Clearfield, A. *Comments Inorg. Chem.* **1990**, *10*, 89.
(44) Ryoo, R.; Kim, J. M.; Ko, C. H.; Shin, C. H. *J. Phys. Chem.* **1996**, *100*, 17718.
(45) Vartuli, J. C.; Schmitt, K. D.; Kresge, C. T.; Roth, W. J.; Leonowicz, M. E.; McCullen, S. B.; Hellring, S. D.; Beck, J. S.; Schlenker, J. L.; Olsen, D. H.; Sheppard, E. W. *Chem. Mater.* **1994**, *6*, 2317.
(46) Gallis, K. W.; Landry, C. C. *Chem. Mater.* **1997**, *9*, 2035.

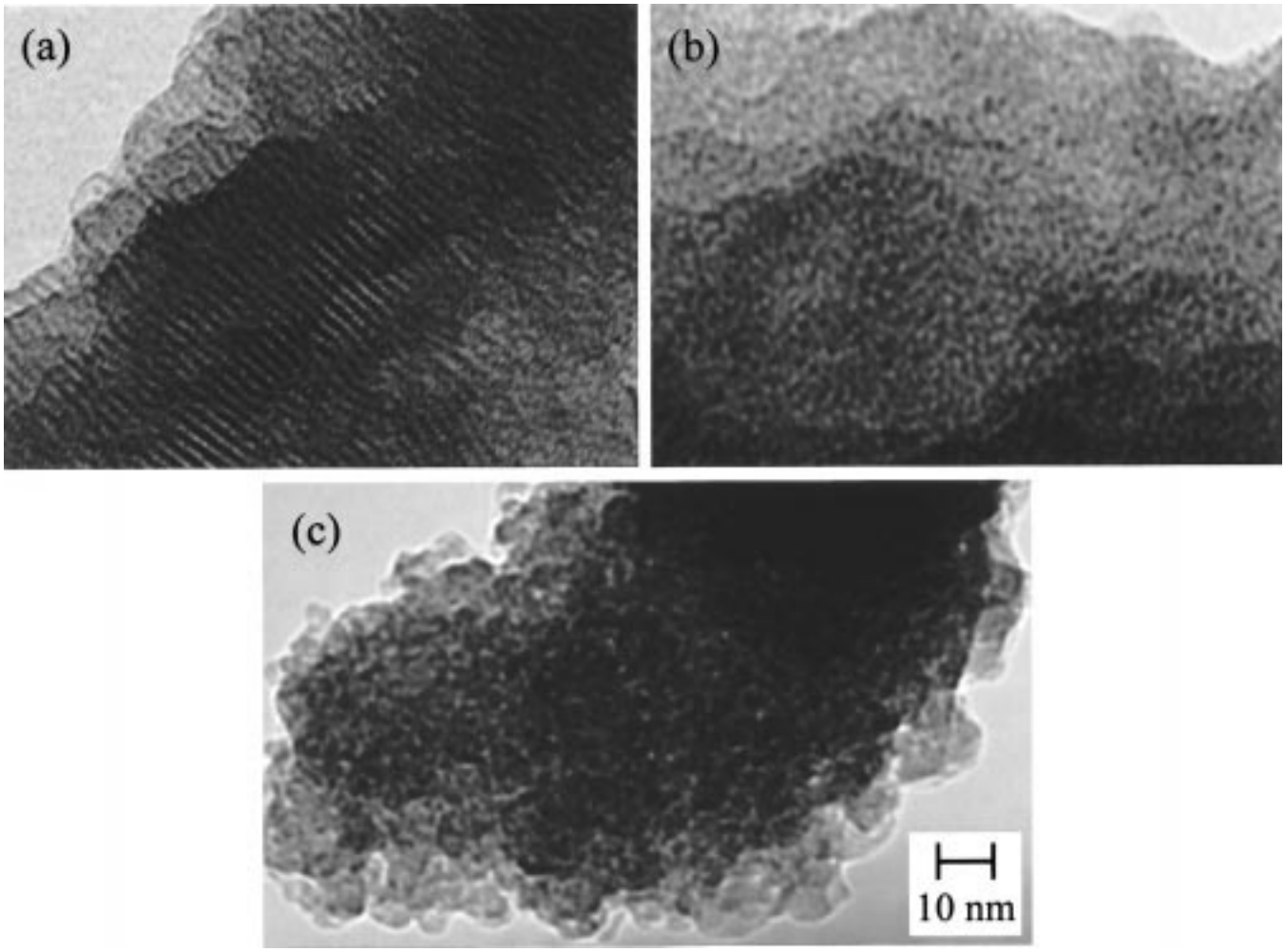

Figure 3. TEM images of (a, b) as-synthesized and (c) calcined Zr-TMS prepared with $C_{12}H_{25}PO_4^{2-}$. All three micrograph images have the same magnification.

XRD patterns of the as-synthesized Zr-TMS materials (Figure 5). Since only the surfactants (which have chain lengths of $n \geq 8$) have typically been used in supramolecular templating, it was interesting to note that an amphiphile as short as four carbons could be successfully used as a templating agent, as evidenced by the XRD pattern of Zr-TMS prepared with $C_4H_9PO_4^{2-}$ (Figure 5a and Table 1). The covalent-bond approach used here and by Sun and Ying[47] enabled the use of very short organic amphiphilic molecules as supramolecular templating agents. In contrast, through the electrostatic approach, the shortest molecule that led to mesostructure formation contained eight carbons in its hydrocarbon tail.[48] To show that the tail group of the alkyl phosphate was necessary for mesostructure formation to occur, orthophosphoric acid (which can be considered an "amphiphile with $n = 0$") was used in place of alkyl phosphates; the resulting material was X-ray amorphous. The addition of solvents for pore swelling had little effect on the d spacings of the mesostructures, another effect of the presence of alcohol in the reaction medium.

Calcination of the series of Zr-TMS materials led to highly porous, X-ray amorphous materials with BET surface areas exceeding 200 m^2/g; the values are listed in Table 2 along with d_{100} spacings (of the precalcined mesostructures), pore volumes, and average pore sizes. The calcined samples prepared with $C_{12}H_{25}PO_4^{2-}$ and $C_{16}H_{33}PO_4^{2-}$ were mesoporous and gave nitrogen adsorption−desorption isotherms (Figure 6c,d) that are type IV with an H2 hysteresis loop; the shape of the isotherms suggested an ink-bottle-type pore structure, rather than a cylindrical pore morphology like that of MCM-41. The type I isotherms of Zr-TMS prepared with $C_4H_9PO_4^{2-}$ and $C_8H_{17}PO_4^{2-}$ indicated microporosity (Figure 6a,b); the average pore sizes could not be determined by applying the BJH method[49] and were estimated, instead, from the electron micrographs of the materials. The pore size distributions of Zr-TMS are broad and not as sharp as that of MCM-41, but the effect of supramolecular templating is clearly manifested in the systematic variation of average pore size, pore volume, and surface area with respect to amphiphile chain length. Removal of the amphiphilic templates was not successful through chemical extraction, indicating that the amphiphile−zirconium interaction is stronger than those typified in hydrogen-bonding and electrostatic interactions.

(47) Sun, T.; Ying, J. Y. *Nature* **1997**, *389*, 704.
(48) Beck, J. S.; Vartuli, J. C.; Kennedy, G. J.; Kresge, C. T.; Roth, W. J.; Schramm, S. E. *Chem. Mater.* **1994**, *6*, 1816.
(49) BJH calculations are based on the Kelvin equation and are limited to pore diameters greater than 17 Å.

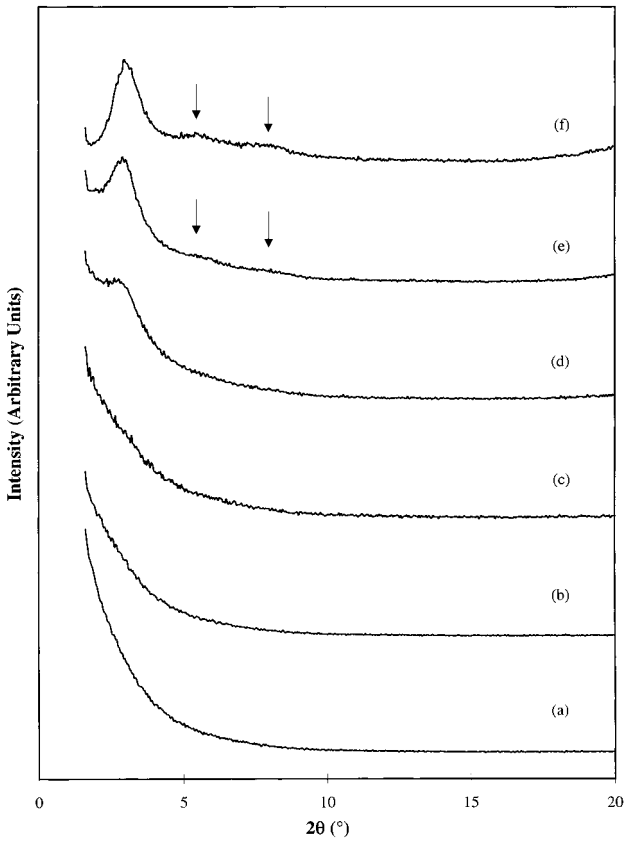

Figure 4. XRD patterns of Zr-TMS prepared with $C_{12}H_{25}PO_4^{2-}$:Zr *n*-propoxide molar ratios of (a) 0.17:1, (b) 0.25:1, (c) 0.50:1, (d) 0.75:1, (e) 1:1, and (f) 2:1. Arrows indicate higher order peaks.

Table 2. Physical Properties of Zr-TMS Prepared with Alkyl Phosphates of Different Chain Lengths

n	d_{100} (Å)[a]	surface area (m^2/g)	avg pore size (Å)	pore volume (cm^3/g)
4	16.6	233	~15	0.208
8	24.2	313	~19	0.227
12	31.0	356	25	0.268
16	38.4	361	26	0.326

[a] As-synthesized samples.

Transmission electron microscopy confirmed that the calcined materials were highly porous. Figure 3c showed that calcined Zr-TMS prepared with $C_{12}H_{25}PO_4^{2-}$ possessed pore sizes ranging from ca. 21 to 32 Å in diameter. On the whole, the pores seemed to be packed together with no visible long-range order, consistent with the absence of low-angle XRD peaks. Zr-TMS was unusual for a surfactant-mediated mesoporous material because it did not exhibit the typical diffraction peaks after surfactant removal and yet it contained very high surface areas and mesoporosity. Its spongelike pore morphology was reminiscent of zirconia aerogels,[30] but its average pore size was substantially smaller, reflecting the micellar dimensions of the amphiphilic templates used in its preparation. As-synthesized, Zr-TMS mesostructures contained a mixture of layered and disordered regions and, after calcination, only disordered, porous regions were noted.

Calcination temperature and purge atmosphere have an important effect on the structure of Zr-TMS materials. Calcination of Zr-TMS prepared with $C_{12}H_{25}PO_4^{2-}$ at 400 °C under air yielded a light beige material with a surface area of ca. 300 m^2/g, but calcination under nitrogen gave a black material of greater than 400 m^2/g. The carbonaceous deposit in the latter amounted to ca. 0.4 wt % and could be removed at 400 °C under air for another 3 h to give a material with a surface area of 356 m^2/g. Careful calcination at 400 °C under vacuum led to even higher surface areas, as reported earlier.[25] Higher calcination temperatures led to decreased surface areas; for example, the BET surface area was found to drop to 300 m^2/g after calcination at 500 °C under N_2. The surface areas obtained after calcination at 600 and 800 °C under air were 103 and 24 m^2/g, respectively. Zr-TMS remained amorphous after calcination at temperatures below 600 °C. Diffraction peaks corresponding to the tetragonal phase of zirconium oxide were noted at 600 °C; typical temperatures for zirconia crystallization to the tetragonal phase are between 400 and 500 °C.

Figure 7 showed PA-FTIR spectra of the as-synthesized and calcined Zr-TMS prepared with $C_{12}H_{25}PO_4^{2-}$, which were representative of Zr-TMS produced with alkyl phosphates. The hydrocarbon deformation and stretching modes (~1400−1500 cm^{-1}, ~2800−3000 cm^{-1}) could be seen in Figure 7a; these bands disappeared after calcination (Figure 7b), indicating the loss of the hydrocarbon tail group. The intense band at ca. 1075 cm^{-1}, assigned to phosphate stretching,[50] was present in both PA-FTIR spectra (with a minor peak shift to 1050 cm^{-1} after calcination), indicating the retention of phosphate anions in the calcined material. The phosphate headgroups were presumed to cover the inner surfaces of the zirconium oxide framework, which would be favorable in terms of enhanced acid strength and catalytic activity for hydrocarbon conversion.[32,43b] The broadening of the phosphate band after calcination also suggested that the chemical environment of the phosphates was different upon calcination. Relative to the phosphate band, the increased intensity of the features below 800 cm^{-1} upon calcination might be a result of further condensation of the zirconium oxide framework. The peak at ca. 1620 cm^{-1} (deformation mode of water) in both spectra indicated the presence of surface adsorbed water, contributing to the broad O−H stretching band above 3100 cm^{-1}. Calcined Zr-TMS was acidic, as both Brønsted and Lewis acid sites were detected through diffuse reflectance infrared Fourier transform (DRIFT) spectroscopic studies with pyridine as the probe molecule. Preliminary studies also showed that the series of Zr-TMS materials was catalytically active for the isomerization of 1-butene to 2-butenes.

A thermogravimetric profile (under air) for Zr-TMS prepared with $C_{12}H_{25}PO_4^{2-}$ was shown in Figure 8. The 2.8% weight loss below 100 °C could be associated with the removal of physisorbed water. A second weight loss of 40.7% occurred between 100 and 400 °C, resulting possibly from the combustion of the hydrocarbon tail group of the amphiphile templating agent. Another 4.6 wt % was lost by 500 °C, which could be attributed to the loss of chemically bound water as the phosphated zirconia framework underwent further condensation and sintering. A total loss of ca. 48 wt % was reached

(50) Busca, G.; Lorenzelli, V.; Galli, P.; La Ginestra, A.; Patrono, P. *J. Chem. Soc., Faraday Trans. 1* **1987**, *83*, 853.

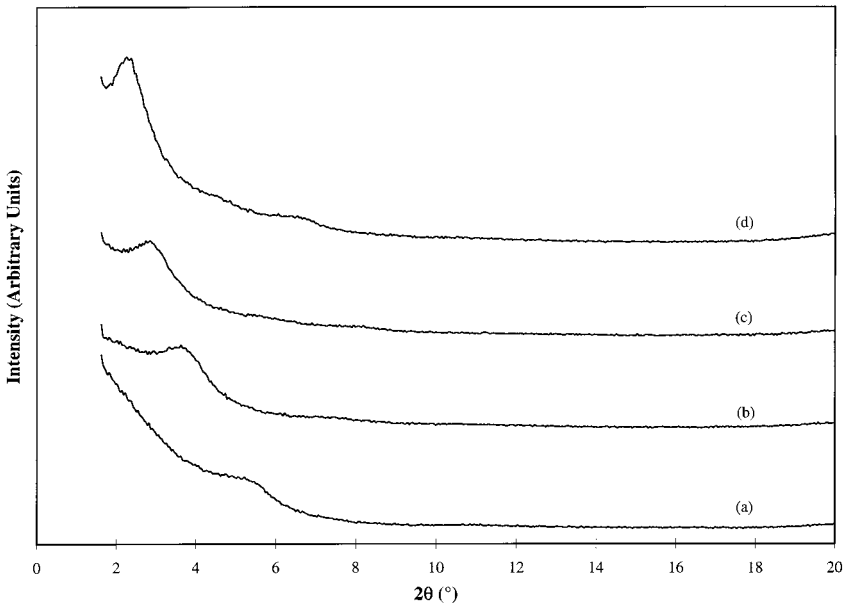

Figure 5. XRD patterns of Zr-TMS prepared with $C_nH_{2n+1}PO_4^{2-}$, with carbon number (n) of (a) 4, (b) 8, (c) 12, and (d) 16.

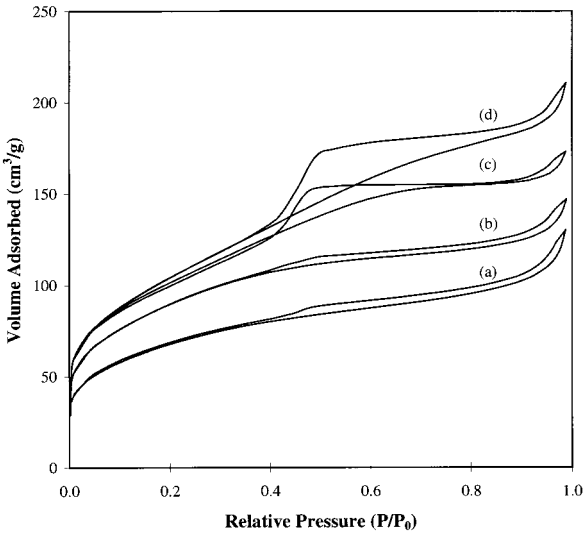

Figure 6. Nitrogen adsorption−desorption isotherms of calcined Zr-TMS prepared with $C_nH_{2n+1}PO_4^{2-}$, with carbon number (n) of (a) 4, (b) 8, (c) 12, and (d) 16.

by 500 °C. On the basis of the assumption that only the tail group of the alkyl phosphate was removed during calcination between 100 and 400 °C, a surfactant:zirconium molar ratio of ca. 1.2:1 was calculated. This ratio was close to the 1.3:1 value derived from elemental analysis of calcined Zr-TMS (32.1 wt % Zr and 13.7 wt % P) and was slightly in excess of the 1:1 ratio used in the synthesis mixture. Similar values from elemental analysis were obtained for Zr-TMS materials synthesized with other alkyl phosphates.

Carboxylate Headgroup. The carboxylate headgroup has two oxygen atoms which can react with the zirconium alkoxide. Not only can the carboxylate functionality form a single bond with the metal but it can chelate to or bridge between multiple zirconium alkoxide molecules à la unidentate and bidentate ligands, respectively,[51] which would be advantageous for mesostructure formation.

(51) Mehrotra, R. C.; Bohra, R. *Metal Carboxylates*; Academic Press: London, 1983.

Carboxylate amphiphiles of varying tail group lengths were combined with zirconium *n*-propoxide to prepare mesostructured zirconium oxide. The effect of chain length on mesostructure formation was readily noted in the XRD patterns of the Zr-TMS materials synthesized with $C_nH_{2n+1}COO^-$ (Figure 9). A systematic shift in the main diffraction peak toward lower 2θ angles was observed, indicating an increase in the d_{100} spacing with increasing length of tail group (Table 1). Secondary diffraction peaks could be seen more distinctly in the materials prepared with longer chain amphiphiles. The *d* spacings of these peaks suggested that these materials might be lamellar in mesostructure, but TEM work only illustrated the presence of large regions of highly packed amphiphile-occluded pores. Carboxylate amphiphiles shorter than eight carbons were not considered as surfactants, but they were found to template mesostructured materials with a distinct (100) peak (Figure 9a−d), as in the case of short-chain phosphate amphiphiles. The formation of mesostructures prepared with amphiphiles of less than eight carbons suggests that the headgroup−inorganic interaction is strong enough to overcome the thermodynamically unfavored micellization of the short-chained amphiphiles. Recovery of an open, mesoporous zirconium oxide framework through carboxylate template removal by calcination or by chemical extraction proved unsuccessful. The materials calcined at 400 °C under air were X-ray amorphous and nonporous, with surface areas less than 30 m^2/g.

Sulfate and Sulfonate Headgroups. Mesostructured zirconium oxide was also prepared from sulfate and sulfonate amphiphiles. Unlike the cases with alkyl phosphates and alkyl carboxylates, the direct combination of the sulfur-containing amphiphile and zirconium *n*-propoxide did not lead to Zr-TMS mesostructures. The headgroups may be too strongly associated with the sodium counterions to interact properly with zirconium *n*-propoxide when dissolved in alcoholic solution.

In a different approach, the amphiphilic compounds were added to an aqueous solution of zirconium acetylacetonate tris(*n*-propoxide) via the modified sol−gel

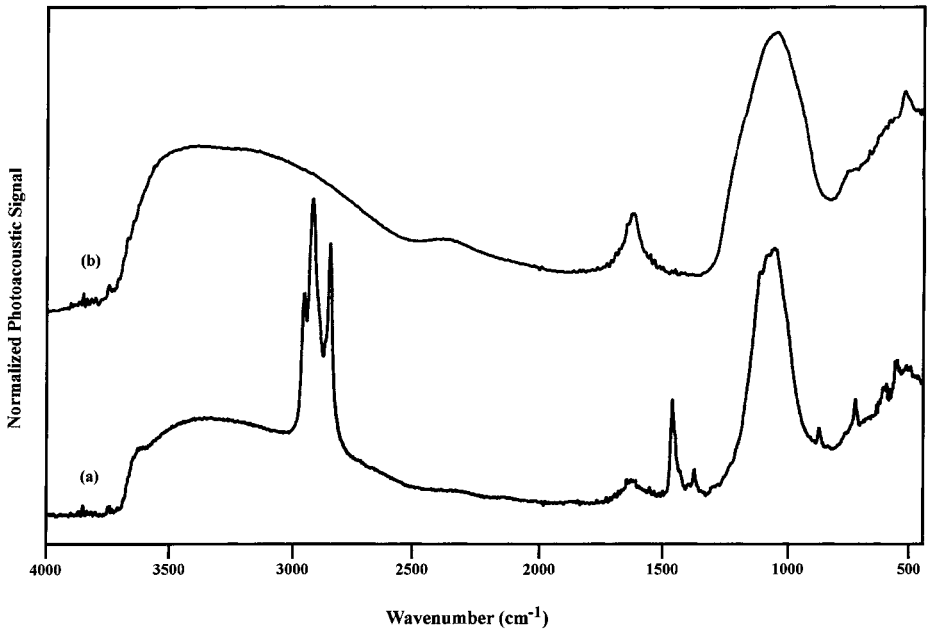

Figure 7. PA-FTIR spectra of (a) as-synthesized and (b) calcined Zr-TMS prepared with $C_{12}H_{25}PO_4^{2-}$. The latter was calcined at 400 °C under nitrogen for 3 h and then under air for 3 h.

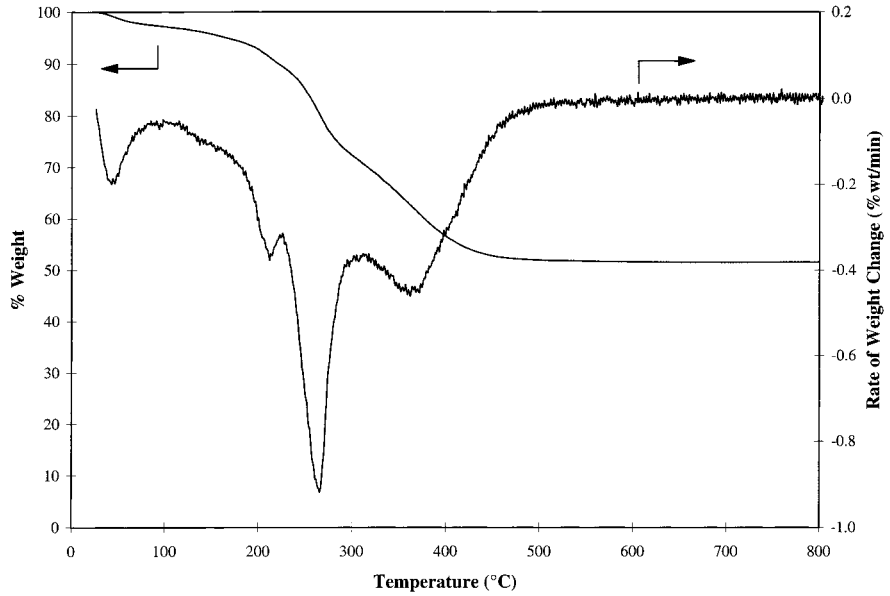

Figure 8. TGA profile and rate of weight change of Zr-TMS prepared with $C_{12}H_{25}PO_4^{2-}$ taken under air.

method. The resulting Zr-TMS mesostructures (Table 1) have lamellar diffraction patterns (Figure 1c,d) and collapsed upon calcination.

Nonionic Amphiphiles. *Amine Headgroup.* Attempts to prepare mesostructured zirconium oxide with the amine amphiphiles were not successful. Both direct-addition and modified sol−gel routes led to materials that appeared X-ray amorphous. The interaction between alkylamines and zirconium *n*-propoxide seemed to be nonexistent within the context of the covalent-bond approach. However, investigation with other types of zirconium alkoxide precursors led to the conclusion that mesostructured zirconium oxide was possible with amine surfactants in the absence of free alcohol. Dodecylamine was warmed until its melting point was reached (28 °C) and zirconium isopropoxide, a solid, was dissolved in it. The resulting solution was heated to 80 °C for 5 min while stirring and then cooled to room temperature before water was added. Aging the mixture at 80 °C for 4 days gave a material with the XRD pattern shown in Figure 1e. With a small broad peak centered around $2\theta = 2.6°$ ($d_{100} = 34.5$ Å, Table 1), this material had a mesostructure that was less well-defined than the Zr-TMS materials prepared with anionic amphiphiles. Zirconium ethoxide led to a similar mesostructure as the former, with $d_{100} = 34.6$ Å; no steric effect associated with the alkoxy ligands was observed. The main difference among the three zirconium alkoxides was the large amount of *n*-propanol present in the zirconium *n*-propoxide precursor. Free alcohol might compete with alkylamines for the coordination sites on the zirconium center and prevent amine ligation if in excess.

Proposed Method of Mesostructure Formation. As the interaction between the metal precursor and the amphiphile headgroup is critical toward mesostructure

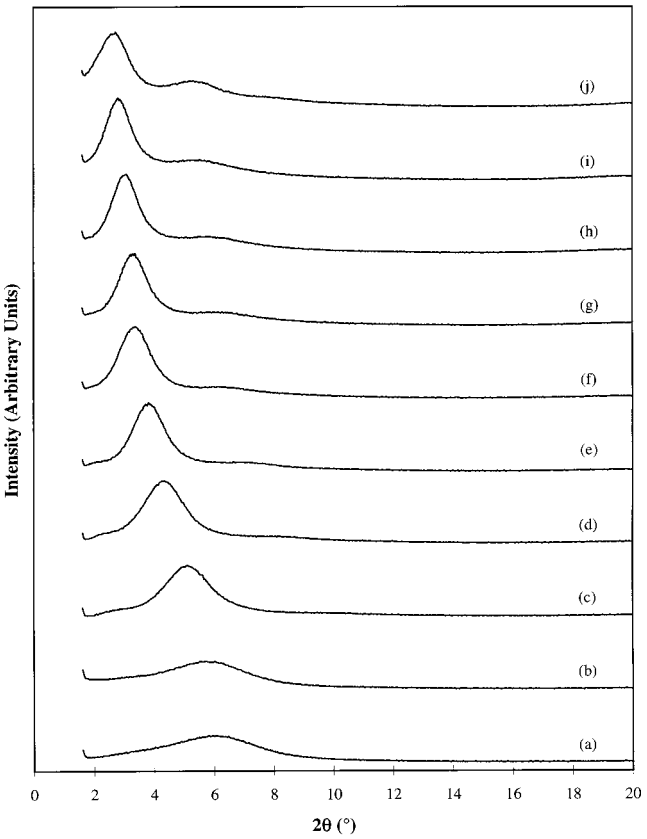

Figure 9. XRD patterns of Zr-TMS prepared with $C_nH_{2n+1}COO^-$, with carbon number (n) of (a) 1, (b) 2, (c) 4, (d) 6, (e) 8, (f) 10, (g) 12, (h) 14, (i) 16, and (j) 18.

formation, we have devised the covalent-bond approach to exploit the strong interaction between the anionic amphiphiles and zirconium *n*-propoxide. Evidence of covalent bonding can be found by examining one of the anionic amphiphiles in particular: dodecyl phosphate. The changes in the chemical environment of the phosphorus in the phosphate headgroup were followed conveniently via ^{31}P MAS NMR. The dihydrogen phosphate surfactant exhibited a slight chemical shift of −0.06 ppm (from phosphoric acid), indicating that the tail group had a negligible effect on the phosphate bonding environment (Figure 10a); the alkyl phosphate headgroup $O(O)P(OH)_2$ was very similar to phosphoric acid $HO(O)P(OH)_2$. The phosphate surfactant in the as-synthesized Zr-TMS mesostructure displayed a dramatically different NMR spectrum (Figure 10b). All the surfactant molecules in Zr-TMS interacted through the headgroup in some manner, as the original peak at −0.06 ppm disappeared and several new peaks emerged in the NMR spectrum. Compared with literature values for phosphorus chemical shifts of crystalline metal(IV) phosphate materials,[52,53] the new peaks might be attributed to two different types of covalent bonding environments with which the phosphate was involved (Table 3). Roughly half of the phosphate headgroups were bound through three oxygens (two hydroxo and one oxo; −20.8 ppm), and the other half were bound through two oxygens (one hydroxo and one oxo; −12.4 and −13.3

(52) Bortun, A. I.; Bortun, L.; Clearfield, A.; Villa-García, M. A.; García, J. R.; Rodríguez, J. *J. Mater. Res.* **1996**, *11*, 2490.
(53) Segawa, K.; Nakajima, Y.; Nakata, S.; Asoaka, S.; Takahashi, H. *J. Catal.* **1986**, *101*, 81.

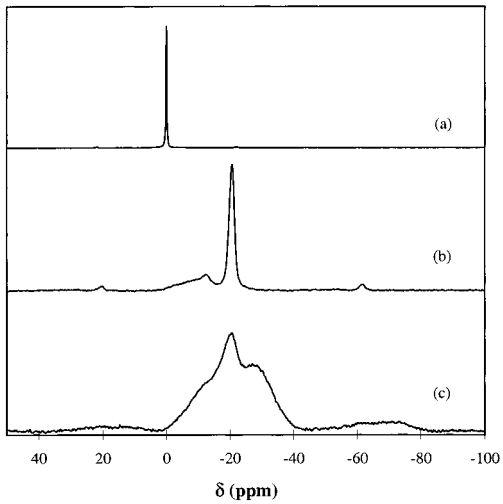

Figure 10. ^{31}P MAS NMR spectra of (a) unreacted $C_{12}H_{25}PO_4^{2-}$ surfactant, (b) as-synthesized Zr-TMS prepared with $C_{12}H_{25}PO_4^{2-}$, and (c) calcined Zr-TMS.

Table 3. ^{31}P NMR Peak Shifts (ppm) of Precalcined and Mesoporous Zr-TMS Materials

		alkyl phosphate	Zr-TMS	
	X = H	(X = $C_{12}H_{23}$)	precalcined	mesoporous
XH_2PO_4	0	−0.06		
$XHPO_4$	−10.6[52]		−12.4 (broad)	−12.4
			−13.3	
XPO_4	−19.3[54]		−20.8	−20.4
PO_4	−32.5[52]			−28.6

ppm), as estimated from the deconvoluted peak areas. The broad peak width around −12.4 ppm suggested a wide distribution of alkyl phosphate bonding environments involving bonding through two oxygens. The phosphate headgroup appeared to have bridged across zirconium cations (through two or three oxygens), similar to the case of α-zirconium phosphate.[43b] This study showed that the phosphate amphiphile (and the other anionic amphiphiles) could be envisioned as a covalently bound ligand to zirconium *n*-propoxide in the mesostructure (Figure 11a).

The method of formation via covalent bonding interactions could be generalized as a schematic in Figure 12 for an anionic amphiphile and zirconium *n*-propoxide. The addition of amphiphile to the zirconium precursor produced oligomers (which might or might not be soluble in *n*-propanol), but because there was no water in the system to drive the micellization process, the oligomers did not self-assemble. Once water was added, hydrolysis and self-assembly processes would occur. The supramolecular aggregates could be of more than one form, such as cylindrical rods and layers; these aggregates combined by condensation at the inorganic−surfactant interface. Aging at an elevated temperature would promote further hydrolysis and condensation of the inorganic framework. If the amphiphile contained the phosphate headgroup, then calcination of the resultant Zr-TMS would yield mesoporous (or microporous) phosphated zirconia.

Nonionic amine surfactants were known to serve as templates for a number of mesoporous materials. Unlike the formation of silicate HMS materials with amine surfactants, which relied on hydrogen-bonding interactions,[34a,c] the formation of mesoporous niobium oxide

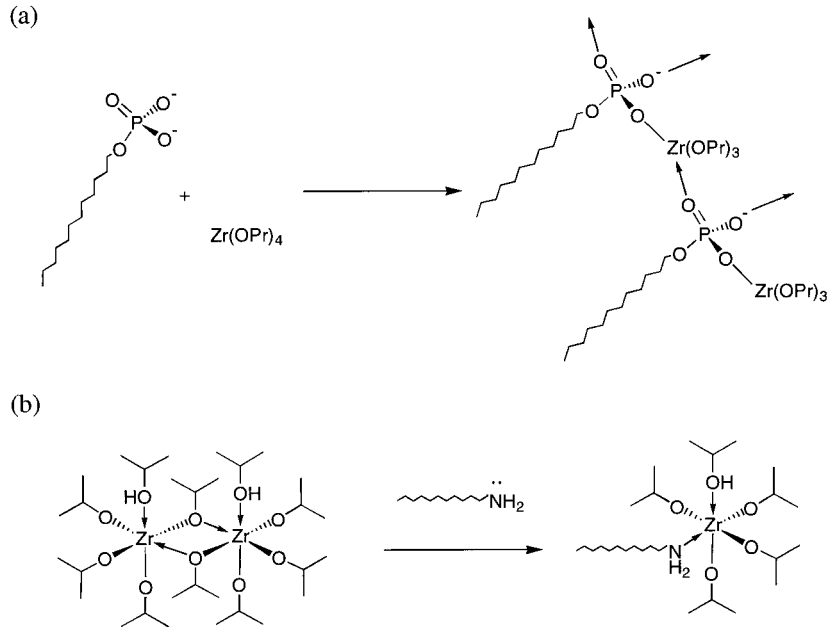

Figure 11. Representative schematic drawings of (a) the anionic amphiphile−zirconium *n*-propoxide interaction, and (b) the nonionic amphiphile−zirconium isopropoxide interaction. The phosphate headgroup in panel a could be substituted by carboxylate (less one reactive oxygen), sulfate, and sulfonate headgroups. Zirconium isopropoxide is shown in dimeric form in panel b.

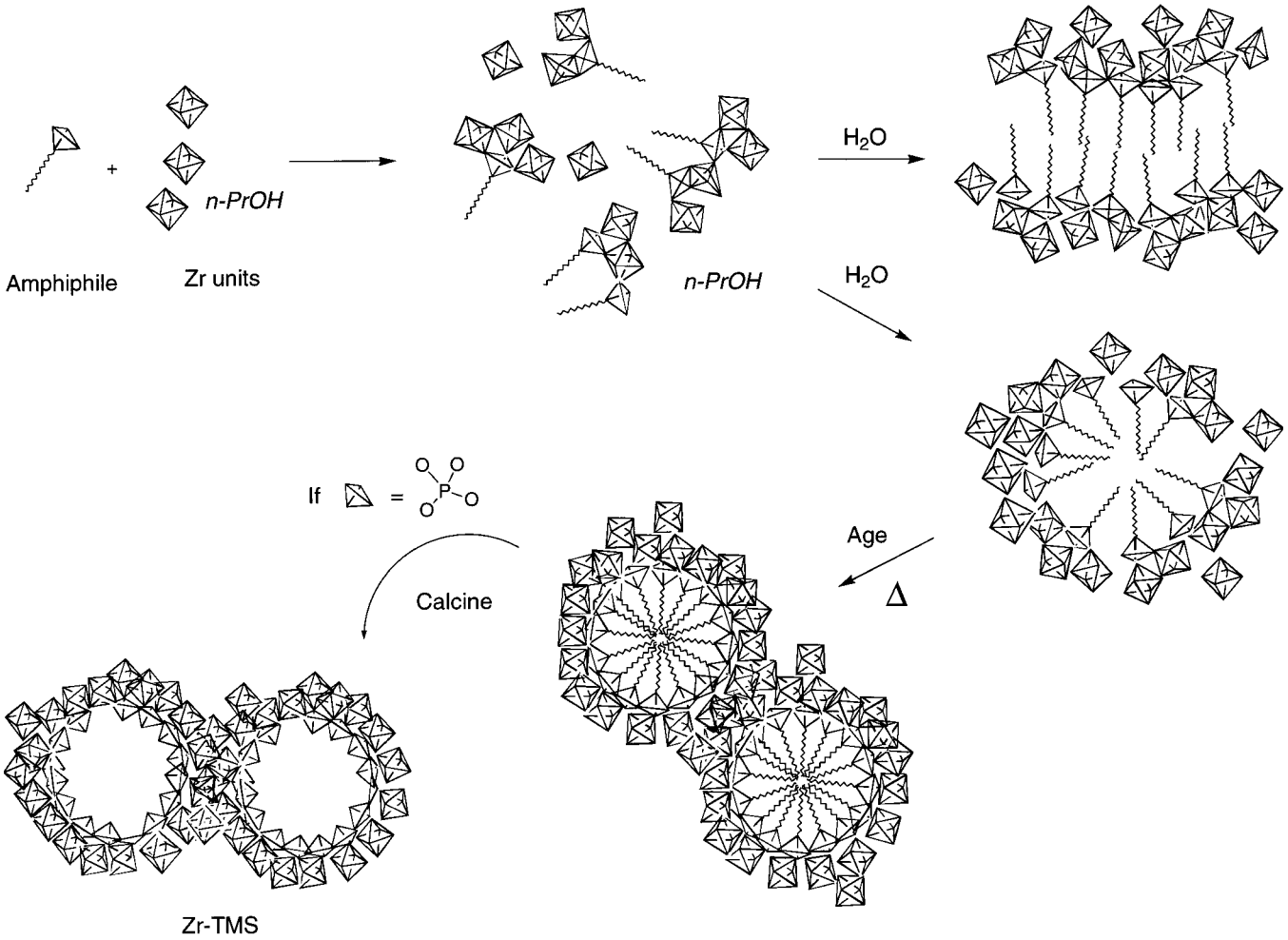

Figure 12. Proposed scheme for the method of Zr-TMS formation with anionic amphiphiles and zirconium *n*-propoxide. The illustrated shapes for the zirconium units and amphiphile were not drawn to scale.

and tantalum oxide TMS1 materials was based upon a strong covalent interaction between the amine surfactant headgroup and the metal alkoxide precursor.[15,17] The "ligand-assisted templating" (LAT) route first developed for the Nb-TMS1 and Ta-TMS1 materials, which was used as the preparative approach for the case

involving the direct addition of amines in this study, was found to give zirconia mesostructures only when the amount of alcohol in the synthesis mixture was minimized (Figure 11b); excess alcohol was found to disrupt mesostructure formation. This contrasted with the preparation of silicate HMS, which required the addition of excess ethanol to the synthesis mixture of alkylamine, tetraethyl orthosilicate, and water.[34a,c]

Stability of Zr-TMS Mesostructures. The removal of the organic templates from mesostructured zirconia did not necessarily lead to mesoporous materials. Only Zr-TMS materials prepared with alkyl phosphates produced highly porous materials upon calcination. The retention of the phosphate headgroups as "molecular braces" fixed along the pore walls appeared to be necessary for the stability of an open porous zirconia framework, as in other surfactant-templated phosphated zirconia.[23,24] Mesostructures prepared with other headgroups would collapse during amphiphile removal, leading to essentially nonporous materials.

The state of the phosphate headgroups in Zr-TMS was very different after calcination (Figure 10c, Table 3). The amount of phosphates that remained in the two- and three-oxygen phosphate bonding environments (−12.4 and −20.4 ppm, respectively) dropped from 50%:50% to 40%:20%, and the remaining 40% appeared in a four-oxygen phosphate bonding environment (−28.6 ppm). With the loss of the tail group, the phosphate headgroup would be able to accommodate another bond to zirconium. The −28.6 ppm peak might represent phosphates within the collapsed layered regions after calcination, suggesting that ∼40% of the Zr-TMS material was layered and unstable to surfactant removal. The broadening of the NMR peaks indicated that the phosphate bonding environments became more anisotropic after calcination, i.e. there was greater variance in the bonding angles of the phosphate anion, consistent with the broadening of the phosphate PA-FTIR band (Figure 7b). The formation of bonds between phosphate headgroups was unlikely due to the absence of NMR peaks at ≤−32 ppm.[54]

Conclusions

Mesostructured zirconia Zr-TMS could be prepared by reacting anionic or nonionic amphiphiles with the zirconium alkoxide prior to the addition of water. Phosphate, carboxylate, sulfate, and sulfonate headgroups have reactive oxygen atoms that could strongly interact with the transition metal, forming the basis for the covalent-bond approach. The amine−zirconium interaction was weaker than the anionic amphiphile−zirconium interactions, and so the covalent-bond approach would not be well-suited for zirconia mesostructure formation with alkylamines. The critical issue of strength of the amphiphile−inorganic interaction was illustrated by the formation of mesostructures templated by amphiphilic molecules with shorter chain lengths than those typical of surfactant molecules. The systematic variation in XRD peak position to changes in amphiphile chain length reflected the supramolecular nature of the templating mechanism and its applicability to amphiphiles regardless of chain length. On the basis of ^{31}P MAS NMR studies of Zr-TMS prepared with dodecyl phosphate, the covalency of the anionic amphiphile−zirconium interaction was further demonstrated and a method of mesostructure formation was proposed. In general, while highly ordered zirconia mesostructures were not retained upon amphiphile removal, high porosity and high surface areas could be achieved from calcination of Zr-TMS templated by alkyl phosphates. Mesoporous and microporous phosphated zirconia materials were obtained, depending on the alkyl chain length of the phosphate amphiphiles used.

Acknowledgment. This work was supported by the National Science Foundation (CTS-9257223, DMR-9400334). The authors thank D. M. Antonelli and T. Sun for helpful discussions.

CM970525Z

(54) Mudrakovskii, I. L.; Shmachkova, V. P.; Kotsarenko, N. S.; Mastikhin, V. M. *J. Phys. Chem. Solids* **1986**, *47*, 335.